IJNRD.ORG ISSN : 2456-4184
INTERNATIONAL JOURNAL OF NOVEL RESEARCH AND DEVELOPMENT (IJNRD) | IJNRD.ORG
An International Open Access, Peer-reviewed, Refereed Journal

Numerical study of MHD convective heat transfer flow of Ethylene Glycol based SWCNT and MWCNT nanofluids in cylindrical annulus with variable viscosity, activation energy

H. Lalramngaihzualí [1] and Prof. D.R.V. Prasada Rao[2]

[1]P.G. Mathematics Student, Mobile : +91 8787327845, Email: lalramngaihzualihlichal@gmail.com

[2]Distinguish Visiting Faculty of Mathematics, Central University of Andhra Pradesh Transit Campus–II, CRIT Campus,Ananthapuramu-505001,Andhra Pradesh,

Abstract : An analysis has been made to investigate the flow of Ethyline Glycole based -Swcnt's and MWcnt's nanofluids in a concentric annular region in the presence of non-uniform heat sources. The non-linear equations have been solved by employing Galerkine finite element method with quadratic polynomials. The velocity, temperature and nano-concentration have been analysed for different parametric values. It is noticed that higher the radiative heat flux(Rd) larger the temperature and concentration, larger with Rd.

Keywords : Circular annulus, Swcnt and Mwcnt-nanofluids, thermal Radiation, Soret effect, chemical reaction, Non-Uniform heat sources

1. INTRODUCTION:

Materials like ethylene glycol, oils and water etc., having low conductivity are less impressive in heat conducting phenomenon.Thermal conductivity and heat transfer coefficient of base materials can be boosted through uinclusion of nanoparticles (Choi and Eastman [8]; Buongiorno [7]. The alignment of solid particles encompassing 1-100 nm size in base materials is known as nanofluids.Investigating approach to enhance heat transportation in engineering utilization for illustration electronic mechanisms chilling equipped with nanofluids, energy stowing structures, heat exchangers, food processing and lubrication equipment employing nanofluids has been examined by numerous scholars.

Reinforcing warming or bracing in an industrial process can save energy, reduce growth time, raise heated rating, and extend equipment life. Increased thermal energy transfer has a qualitative effect on several processes. The development of high-performance thermal systems for heat transfer enrichment has recently gained popularity. A lot of studies have been conducted to get a better knowledge of thermal energy transfer enforcement for experimental applications in heat transfer improvement. As a result, the creation of high heat flow has piqued the interest of new researchers in heat transfer enhancement. Single-walled carbon nanotubes (SWCNTs), a member of the carbon family, are one-dimensional equivalents of zero-dimensional falling molecules with unusual structural and electrical characteristics. Single-walled nanotubes are the most likely choice for miniaturizing electronics beyond the microelectrothermal scale now used in electronics. Carbon nanotubes (CNTs) have received a lot of interest because to their linear model and significant mechanical, thermal, and electrical properties (Al-Marri et al. [3], Arash Karimipour et. Al. [5], Maria Imtiaz et al. [14], Mehdi Nojoomizadeh and Arash Karimipour [15], Shahsavar et al. [20]). CNTs have been employed as liquid preservatives to improve thermal energy conductivity, which is a critical issue in industry. With these qualities, nanofluids look to have interesting applications in industries such as heat exchangers. Anyway, the development and uses of nanofluids may be hampered by numerous aspects, such as increasing state durability, pushing force, and pressure.

The study for thermophysical properties of CNTs nanofluids with base fluid as mixture of water and ethylene glycol has been presented by Kumaresan and Velraj [13]. And this study noted that the maximum thermal conductivity enhances up to 19.75% for the nanofluid containing 0.45 vol.% MWCNT at 40°C. The entropy generation Berrehal [6], Shafiq et al [19] CNT'S are rolled–up grapheme sheets arranged in a cylindrical shape. They are of two types single walled (SWCNT's)) and multi-walled (MWCNT's). Kamali and Binesh [10] numerically investigated the convective heat transfer of multi-wall carbon nano-tube (MWCNT)-based nanofluids in a straight tube under constant wall heat flux condition. They solved Navier-Stokes equations using the finite volume technique considering CNT-based nanofluids using power law model. Vijayalakshmi [24] has considered the hydromagnetic convective heat transfer flow of Swcnt-water nanofluid in a circular annuls. Kiran Kumar et.al.[12] have described the effect of thermal radiation on nonDarcy hydromagnetic convective heat and mass transfer flow of a water -SWCNT's and MWCNT's nanofluids in a cylindrical annulus with thermo-diffusion and chemical reaction.

In chemistry and physics, activation energy is the minimum amount of energy that must be provided for compounds to result in a chemical reaction. The activation energy (*Ea*) of a reaction is measured in joules per mole (J/mol), kilojoules per mole (kJ/mol) or kilocalories per mole (kcal/mol). Activation energy can be thought of as the magnitude of the potential

barrier (sometimes called the energy barrier) separating minima of the potential energy surface pertaining to the initial and final thermodynamic state. For a chemical reaction to proceed at a reasonable rate, the temperature of the system should be high enough such that there exists an appreciable number of molecules with translational energy equal to or greater than the activation energy. The term "activation energy" was introduced in 1889 by the Swedish scientist Svante Arrhenius.[21]. The Natural convection of the nanofluid in a concentric annulus with variable viscosity and thermal conductivity is studied by AbuNada et al.[1] and Abu-Nada[2]. The several authors have been analyzed about activation energy like, Amitosh Tiwari et al [4] have been discussion to activation energy impacts on hydromagnetic convective heat transfer flow of nanofluid past a surface of vertical wavy with variable properties. Kathyani and Subramanyam[11] have explored the effect of activation energy on thermally radiative, dissipative electrically conducting, viscous fluid flow in a vertical channel in the presence of heat sources. Several authors (Satya Narayana and Ramakrishna[18], Nagasasikala [16], Devasena [9] have demonstrated the influence of activation energy on flow phenomenon.

The objective of this study is to investigate and highlight the effect of thermal radiation and heat source effect on convective heat transfer flow of Swcnt-water and Mwcnt-Eg nanofluids in the case of concentric annulus. This is performed by employing a theoretical mathematical model, previously introduced by Tiwari and Das [23]. Their model presented the effect of nanoparticles volume fraction in influencing the viscosity of nanofluid.The behaviour of velocity, temperature and concentration is analyze d at different axial positions. The shear stress and the rate of heat and mass transfer have also been obtained for variations in the governing parameters.

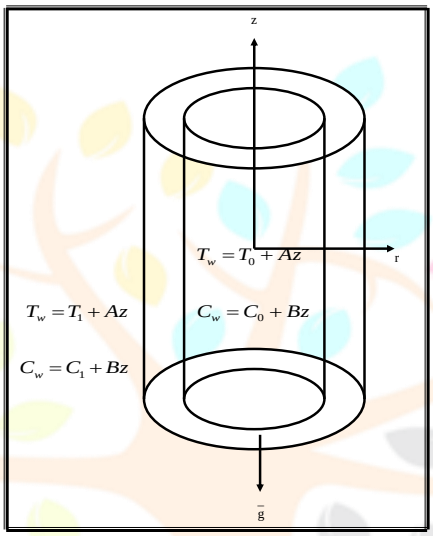

Fig.1 : CONFIGURATION OF THE PROBLEM

2. FORMULATION OF THE PROBLEM:

We analyse the mixed convective flow of a SWCNt-water and Mwcnt-water nanofluids in a vertical circular annulus through a porous medium whose walls are maintained at a constant heat and concentration. The flow, temperature and concentration in the fluid are assumed to be fully developed. Both the fluid and porous region have constant physical properties and the flow is a mixed convection flow taking place under thermal and molecular buoyancies and uniform axial pressure gradient. The Boussinesq approximation is invoked so that the density variation is confined to the thermal and molecular buoyancy forces. The Brinkman-Forchheimer-Extended Darcy model which accounts for the inertia and boundary effects has been used for the momentum equation in the porous region. The momentum, energy and diffusion equations are coupled and non-linear. Also the flow is unidirectional along the axial direction of the cylindrical annulus. Making use of the above assumptions the governing equations are

$$-\frac{\partial p}{\partial z}+\frac{1}{\rho_{nf}\delta r}\frac{\partial}{\partial r}\left((\mu_{nf}(T)\,\mathrm{r}\frac{\partial u}{\partial r})\right)-(\frac{\mu_{nf}}{\rho_{nf}k})u-\frac{\sigma_f(T)\mu_e^2H_0^2}{\rho_{nf}r^2}-\frac{\delta F}{\rho_{nf}\sqrt{k}}u^2+(\rho\beta)_{nf}(T-T_o)=0 \quad (2.1)$$

$$(\rho C_p)_{nf}\,u\frac{\partial T}{\partial z}=k_{nf}(\frac{\partial^2 T}{\partial r^2}+\frac{1}{r}\frac{\partial T}{\partial r})+q'''-\frac{1}{r}\frac{\partial(rq_r)}{\partial r}+Q_1^{'}(C-C_0) \quad (2.2)$$

$$u\frac{\partial C}{\partial z}=D_B\left(\frac{\partial^2 C}{\partial r^2}+\frac{1}{r}\frac{\partial C}{\partial r}\right)-k_c^{'}C+\frac{D_mK_T}{T_s}\left(\frac{\partial^2 T}{\partial r^2}+\frac{1}{r}\frac{\partial T}{\partial r}\right)- \quad (2.3)$$

$$-kc(\mathrm{C}-\mathrm{C}_0)(\frac{T}{T_o})^n Exp(-\frac{E_a}{KT})$$

where u is the axial velocity in the porous region, T , C are the temperature and concentration of the fluid, k is the permeability of porous medium, k_f is the thermal diffusivity, F is a function that depends on Reynolds number, the microstructure of the porous medium and D_B is the molecular diffusivity, D_m is the mass diffusivity, K_T mass diffusion ratio, β is the coefficient of the thermal expansion, q_R is the radiation absorption coefficient, Cp is the specific heat, ρ is density ,g is gravity, ρ_{nf} is the effective density . μ_{nf} is the effective dynamic viscosity, k_{nf} is the thermal conductivity of the nanofluid.

The relevant boundary conditions are

$u=0$, T=T_w , C=C_w at r = a&a+s (2.4)

Following Tao [22], we assume that the temperature and concentration of the both walls is $T_w = T_0 + Az$, $C_w = C_0 + Bz$ where A and B are the vertical temperature and concentration gradients which are positive for buoyancy –aided flow and negative for buoyancy – opposed flow, respectively, T_0 and C_0 are the upstream reference wall temperature and concentration ,respectively.

The coefficient q''' is the rate of internal heat generation (>0) or absorption(<0). The internal heat generation /absorption q''' is modelled as

$$q''' = (\frac{k_f}{a^2 \nu})(A^\bullet (T_w - T_0)u + B^\bullet (T - T_0)) \quad (2.5)$$

Where $A^\bullet$ and $B^\bullet$ are coefficients of space dependent and temperature dependent internal heat generation or absorption respectively. It is noted that the case $A^\bullet$>0 and $B^\bullet$>0, corresponds to internal heat generation and that $A^\bullet$<0 and $B^\bullet$<0, the case corresponds to internal heat absorption case.

We now define the following non-dimensional variables for the fully developed laminar flow in the presences of radial magnetic field, the velocity depend only on the radial coordinate and all the other physical variables except temperature, concentration and pressure are functions of r and z, z being the vertical co-ordinate .The temperature and concentration inside the fluid can be written as

$$T = T^\bullet (r) + Az \quad , \quad C = C^\bullet (r) + Bz \quad (2.6)$$

The effective density of the nanofluid is given by

$$\rho_{nf} = (1-\varphi)\rho_f + \varphi\rho_s \quad (2.7)$$

Where ϕ is the solid volume fraction of nanoparticles. Thermal diffusivity of the nanofluid is

$$\alpha_{nf} = \frac{k_{nf}}{(\rho C_p)_{nf}} \quad (2.8)$$

Where the heat capacitance C_p of the nanofluid is obtained as

$$(\rho C_p)_{nf} = (1-\varphi)(\rho C_p)_f + \varphi(\rho C_p)_s \quad (2.9)$$

And the thermal conductivity of the nanofluid k_{nf} for spherical nanoparticles can be written as

$$\frac{k_{nf}}{k_f} = \frac{(k_s + 2k_f) - 2\phi(k_f - k_s)}{(k_s + 2k_f) + \phi(k_f - k_s)} \quad (2.10)$$

The thermal expansion coefficient of nanofluid can determine by

$$(\rho\beta)_{nf} = (1-\varphi)(\rho\beta)_f + \varphi(\rho\beta)_s \quad (2.11)$$

Also the effective dynamic viscosity of the nanofluid given by

$$\mu_{nf} = \frac{\mu_f}{(1-\varphi)^{2.5}}, \ \sigma_{nf} = \sigma_f (1 + \frac{3(\sigma-1)\phi}{\sigma + 2 - (\sigma-1)\phi}), \sigma = \frac{\sigma_s}{\sigma_f} \quad (2.12)$$

Where the subscripts nf, f and s represent the thermo physical properties of the nanofluid, base fluid and the nanosolid particles respectively and ϕ is the solid volume fraction of the nanoparticles. The thermo physical properties of the nanofluid are given in Table 1.

The thermo physical properties of the nanofluids are given in Table 1 (See Oztop and Abu-Nada [17]).

Table – 1

Physical properties	Fluid phase (Eg)	**Swcnt's**	**Mwcnt's**
C_p(j/kg K)	**1115**	**425**	**796**
ρ(kg m^3)	2430	**2600**	**1600**
k(W/m K)	0.253	**6600**	**3000**
βx10^{-5} 1/k)	5.7	2.0	**2.0**
σ	**10.7**	**10^6**	**10^7**

We now define the following non-dimensional variables

$$z^* = \frac{z}{a} \quad , \quad r^* = \frac{r}{a} \quad , \quad u^* = (\frac{a}{\nu})u \ , \ p^* = \frac{pa\delta}{\rho\nu^2} \ ,$$

$$\theta^*(r^\bullet) = \frac{T^\bullet - T_0}{P_1 Aa} \quad , \quad C^*(r^\bullet) = \frac{C^\bullet - C_0}{P_1 Ba} \ , \ s^* = \frac{s}{a}, P_1 = \frac{dp}{dx} \quad (2.13)$$

Introducing these non-dimensional variables, the governing equations in the non-dimensional form are (on removing the stars)

$$(\frac{\partial^2 u}{\partial r^2} + \frac{1}{r}\frac{\partial u}{\partial r} - \mathrm{B}(\frac{\partial u}{\partial r})(\frac{\partial T}{\partial r})) = A_1 A_3 \mathrm{e}^{B\theta} + \delta A_1 (D^{-1} + \frac{A_6 M^2 \mathrm{e}^{B\theta}}{r^2})u + \delta A_1 A_4 G \mathrm{e}^{B\theta}(\theta) \quad (2.14)$$

$$A_2 (1 + \frac{4Rd}{3})(\frac{\partial^2 \theta}{\partial r^2} + \frac{1}{r}\frac{\partial \theta}{\partial r}) + (A1u + B1\theta) + Q_1 C = A_5 \,\mathrm{Pr}\, u \quad (2.15)$$

$$(\frac{\partial^2 C}{\partial r^2}+\frac{1}{r}\frac{\partial C}{\partial r})-\gamma C = Sc\,u + ScSr\left(\frac{\partial^2\theta}{\partial r^2}+\frac{1}{r}\frac{\partial\theta}{\partial r}\right)-\gamma C(1+n\delta\theta)Exp(-\frac{E_1}{1+\delta\theta}) \qquad (2.16)$$

where

$B = m(T_0 - T_i)$ (Viscosity parameter)

$\Delta = FD^{-1/2}$ (Inertia parameter or Forchheimer number)

$G = \frac{g\beta(T_e - T_i)a^3}{\nu^2}$ (Grashof number), $M^2 = \frac{\sigma\mu_e^2 H_0^2}{a\nu}$ (magnetic parameter), $D^{-1} = \frac{a^2}{k}$ (Inverse Darcy parameter),

$P_r = \frac{\mu C_p}{k_f}$ (Prandtl number), $Rd = \frac{4\sigma^{\bullet}T_o^3}{k_f\beta_R}$ (Thermal radiation parameter), $Sc = \frac{\nu}{D_B}$ (Schmidt number), $\gamma = \frac{k_c a^2}{D_B}$

(Chemical Reaction parameter), $So = \frac{D_m K_T(T_0 - T_{i)}}{T_s(C_0 - C_i)}$ (Soret parameter), $Q_1 = \frac{Q_1^{'}(C_w - C_0)}{a^2(T_w - T_0)}$ (Radiation absorption

parameter), $\theta_w = \frac{T}{T_o}$, $\delta = \theta_w - 1$, Temperature difference ratio, $E_1 = \frac{E_a}{KT_0}$ (Activation energy parameter)

$A_1 = \frac{1}{(1-\varphi)^{2.5}}$, $A_2 = (1-\varphi)+\varphi(\frac{\rho_s}{\rho_f})$ $A_1 = \frac{1}{(1-\varphi)^{2.5}}$, $A_2 = (1-\varphi)+\varphi(\frac{\rho_s}{\rho_f})$, $A_3 = 1-\varphi+\varphi\frac{(\rho C_p)_s}{(\rho C_p)_f}$,

$A_4 = 1-\varphi+\varphi(\frac{(\rho\beta)_s}{(\rho\beta)_f}$, $A_5 = \frac{k_{nf}}{k_f}$ $A_6 = (1+\frac{3(\sigma-1)}{\sigma+2-(\sigma-1)\phi}), \sigma_{nf} = \sigma_f A_6, \sigma = \frac{\sigma_s}{\sigma_f}$

The corresponding non-dimensional conditions are

$u = 0 \quad \theta = 0$ C=0 at r=1 and 1+s (2.17)

3. METHOD OF SOLUTION (Finite Element Analysis**)**

The finite element analysis with quadratic polynomial approximation functions is carried out along the radial distance across the circular duct. The behavior of the velocity, temperature and concentration profiles has been discussed computationally for different variations in governing parameters. The Galerkin method has been adopted in the variational formulation in each element to obtain the global coupled matrices for the velocity, temperature and concentration in course of the finite element analysis.

Choose an arbitrary element e_k and let u^k, θ^k and C^k be the values of u, θ and C in the element e_k. We define the error residuals as

$$E_p^k = \frac{d}{dr}\left(r\frac{du^k}{dr}\right)-B(\frac{du^k}{dr})(\frac{d\theta^k}{dr})+\delta A_1A_4rG\,e^{B\theta^k}(\theta^k)-\delta A_1(D^{-1}+\frac{A_6M^2e^{B\theta^k}}{r^2})ru^k-A_1A_3e^{B\theta^k} \qquad (3.1)$$

$$E^k{}_\theta = \frac{A_2}{\Pr}(1+\frac{4Rd}{3})\frac{d}{dr}\left(r\frac{d\theta^k}{dr}\right)-A_5ru^k+(A_1u^k+B_1\theta^k)+Q_1C^k \qquad (3.2)$$

$$E^k{}_c = \frac{d}{dr}\left(r\frac{dC^k}{dr}\right)-rScu^k-\gamma C^k+ScS_r\frac{d}{dr}\left(r\frac{d\theta^k}{dr}\right)-\gamma C^k(1+n\delta\theta^k)Exp(-\frac{E_1}{1+\delta\theta^k}) \qquad (3.3)$$

where u^k, θ^k & C^k are values of u, θ& C in the arbitrary element e_k. These are expressed as linear combinations in terms of respective local nodal values.

$$u^k = u_1^k\psi_1^k + u_2^k\psi_1^k + u_3^k\psi_3^k$$
$$\theta^k = \theta_1^k\psi_1^k + \theta_2^k\psi_2^k + \theta_3^k\psi_3^k$$
$$C^k = C_1^k\psi_1^k + C_2^k\psi_2^k + C_3^k\psi_3^k$$

where ψ_1^k, ψ_2^k --------- etc are Lagrange's quadratic polynomials.

Galarkin's method is used to convert the partial differential Equations (3.1) – (3.3) into matrix form of equations which results into 3x3 local stiffness matrices. All these local matrices are assembled in a global matrix by substituting the global nodal values and using inter element continuity and equilibrium conditions. The resulting global matrices have solved by iterative procedure until the convergence i.e $|u_{i+1}-u_i|<10^{-6}$ is obtained.

4. SHEAR STRESS,NUSSELT NUMBER AND SHERWOOD NUMBER

The shear stress (τ) is evaluated using the formula $\tau = (\frac{du}{dr})_{r=1,1+s}$.

The rate of heat transfer (Nusselt number) is evaluated using the formula $Nu = -(\frac{d\theta}{dr})_{r=1,1+s}$.

The rate of mass transfer (Sherwood number) is evaluated using the formula $Sh = -(\frac{dC}{dr})_{r=1,1+s}$

5. COMPARISON

In the absence of activation energy (E1=0) & variable viscosity (B=0) .The results are good agree with Kiran Kumar et.al.[12]

Table – 2

Parameter		Kiran Kumar et.al.[12] results		**Present Results**		Kiran Kumar et.al.[12] results		**Present Results**	
		Eg-Swcnt				Eg-Mwcnt			
		τ(1)	Nu(1)	τ(1)	Nu(1)	τ(1)	Nu(1)	τ(1)	Nu(1)
Rd	0.5	-0.167074	0.999968	-0.502712	-0.184469	-0.102191	0.999955	-0.502928	-0.405918
	1.5	-0.167076	0.999993	-0.502714	-0.102477	-0.102193	0.999975	-0.502927	-0.225483
	3.5	-0.167084	0.999996	-0.502716	-0.040093	-0.102194	0.999987	-0.502930	-0.088787
	5	-0.167165	0.999997	-0.502718	-0.020087	-0.102195	0.99999	-0.503000	-0.066888
Ec	0.01	-0.334342	0.999954	-0.502712	-0.184469	-0.102191	0.999955	-0.502928	-0.405918
	0.03	-0.167074	0.999965	-0.502706	-0.304786	-0.102190	0.999951	-0.502914	-0.670669
	0.05	-0.011655	0.999975	-0.502697	-0.425090	-0.102188	0.999947	-0.502892	-0.943638
	0.07	-0.010458	0.999976	-0.502588	-0.518722	-0.102179	0.999942	-0.502688	-0.178298
ϕ	0.05	-0.167074	0.999968	-0.502712	-0.184469	-0.460268	0.999883	-0.502928	-0.405918
	0.10	-0.198163	0.999966	-0.503538	-0.185328	-0.460244	0.999879	-0.503973	-0.407908
	0.15	-0.244968	0.999963	-0.504146	-0.186028	-0.464207	0.999882	-0.504802	-0.412275
	0.20	-0.300647	0.999958	-0.505064	-0.187215	-0.470861	0.999877	-0.505176	-0.421433

6. NUMERICAL RESULTS AND DISCUSSION:

The equations governing the flow,heat and mass transfer flow Water based Swcnt and Mwcnt nanofluids have been solved by employing Galerkine kinite element analysis with quadratic approximation polynomials.We have chosen here Pr=6.2 while Rd, Ec, B, E1, A11, B11 and δ are varied over a range, which are listed in the Figure legends.

In this analysis, we explore the combine influence of heat sources / activation energy/Thermal radiation/variable viscosity on hydromagnetic convective heat transfer flow of Ethylene Glycol base Swcnt and Mwcnt nanofluids to a porous medium in vertical channel. The resulting non-linear coupled equations have been solved by finite element measure with a quadratic interpolation functions. The velocity, temperature nano-concentration are exhibited for different parameter variation in figs. The skin fraction, rate of heat and mass transfer on the wall has been evaluated numerically.

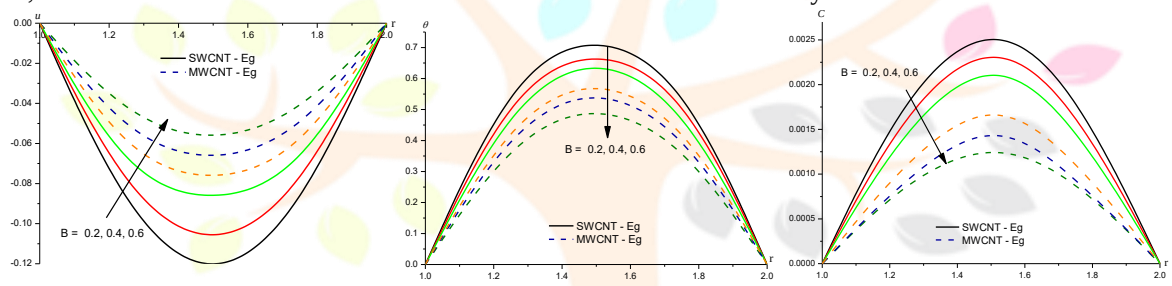

Fig.2 : Variation of [a] Velocity (*u*), [b] Temperature(θ), [c] Nanoconcentration(C) with B
Rd=0.5, Ec=0.1, A11=0.1, B11=0.5 E1=0.1, δ=0.1

Figs. 2(a)-2(c) represent the variation of the flow variables (u,θ,c) with variable viscosity parameter 'B'. From the profiles we find that for higher values of viscosity parameter 'B' we notice a depreciation in (u,θ,c) in all the nanofluid.This maybe due to the fact that with increase in 'B' the momentum, thermal and the boundary layer becomes thinner. The values of (u,θ,c) in Eg-Swcnt case are relatively higher than those in Eg-Mwcnt case.

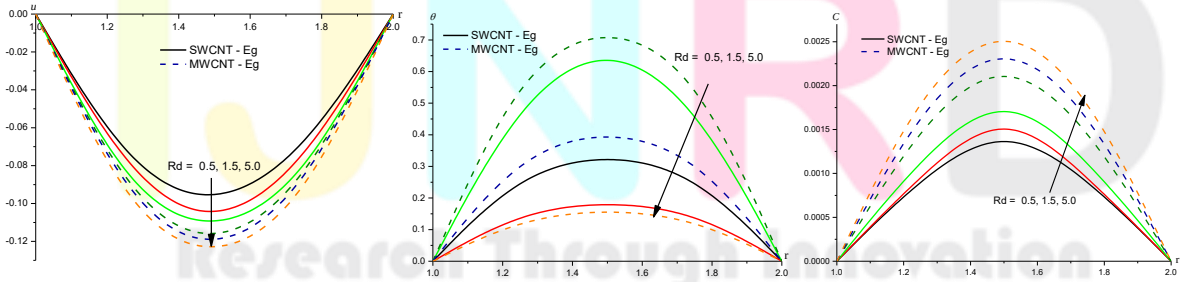

Fig.3 : Variation of [a] Velocity (*u*), [b] Temperature(θ), [c] Nanoconcentration(C) with Rd
Ec=0.1, A11=0.1, B11=0.5, B=0.2, E1=0.1, δ=0.1

The effect of thermal radiation on (u,θ,c) can be absorbed from figs. 3(a)-3(c) fixed in the other parameters. From figure 3(a) & 3(c) we find that magnitude of velocity and nanoconcentration 'C' grow with higher values of radiation parameter (Rd) while the temperature experiences reduction with 'Rd'.The momentum and solutal boundary layers thicker and thermal boundary layer become thinner with rising values of 'Rd'. From the figures we also find that the values of flow variables (u,θ,c) in Eg-Swcnt case are relatively smaller than those in Eg-Mwcnt case.

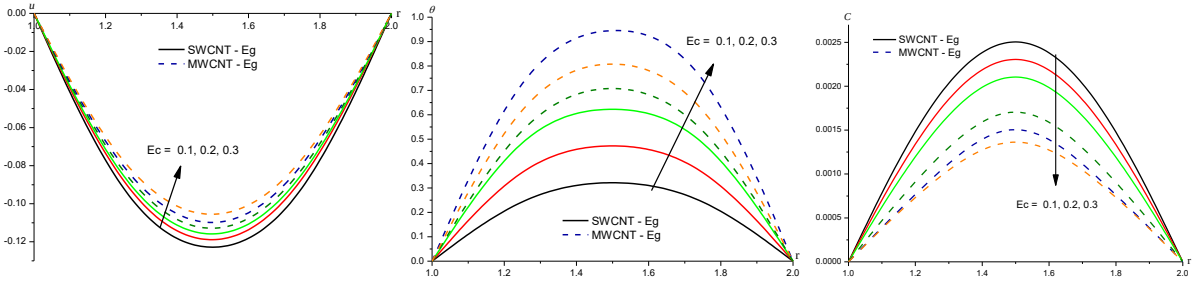

Fig.4 : Variation of [a] Velocity (u), [b] Temperature(θ), [c] Nanoconcentration(C) with Ec
Rd=0.5, A11=0.1, B11=0.5, B=0.2, E1=0.1, δ=0.1

Figs. 4(a)-4(c) demonstrate the influence of viscosity dissipation (Ec) on (u,θ,c). Higher the dissipative energy smaller the magnitude of velocity and nanoconcentration and larger the temperature dissipation in the flow region. This maybe due to the fact that the momentum solutal boundary layer becomes thinner and thermal boundary layer become thicker with increased in values of 'Ec'.The values of velocity and concentration in Eg-Swcnt case are relatively greater than those in Eg-Mwcnt case while an opposite effect is observed in the case of temperature.

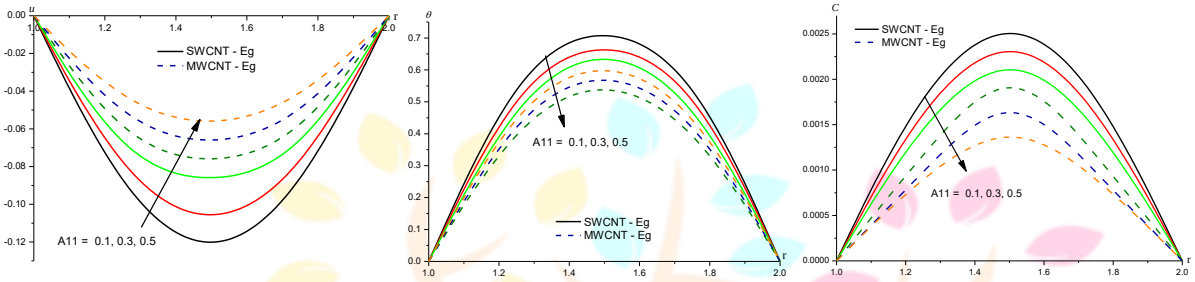

Fig.5 : Variation of [a] Velocity (u), [b] Temperature(θ), [c] Nanoconcentration(C) with A11
Rd=0.5, Ec=0.1, B11=0.5, B=0.2, E1=0.1, δ=0.1

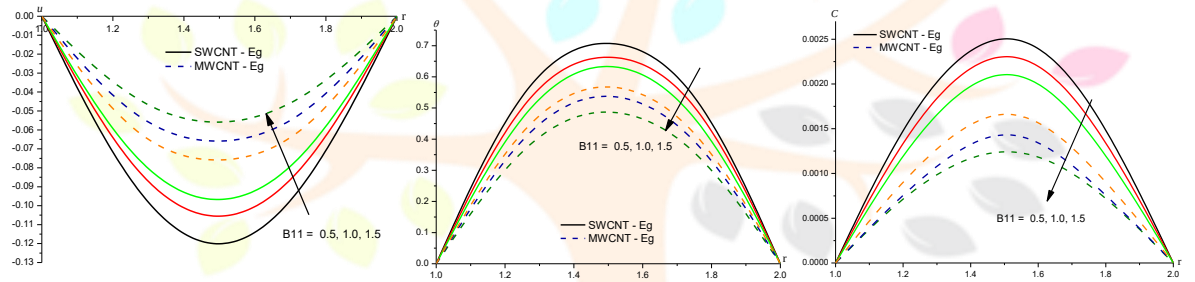

Fig.6 : Variation of [a] Velocity (u), [b] Temperature(θ), [c] Nanoconcentration(C) with B11
Rd=0.5, Ec=0.1A11=0.1, B=0.2, E1=0.1, δ=0.1

Figs. 5(a)-5(c)/figs. 6(a)-6(c) represent variation of (u,θ,c) / temperature dependent heat sources.The velocity, temperature, nanoconcentration experienced the depreciation with rising values of A11/B11. The momentum thermal and boundary layer becomes thinner with larger values of A11/B11. Also we notice that the values of velocity temperature nanoconcentration in Eg-Swcnt case are relatively higher than those in Eg-Mwcnt case.

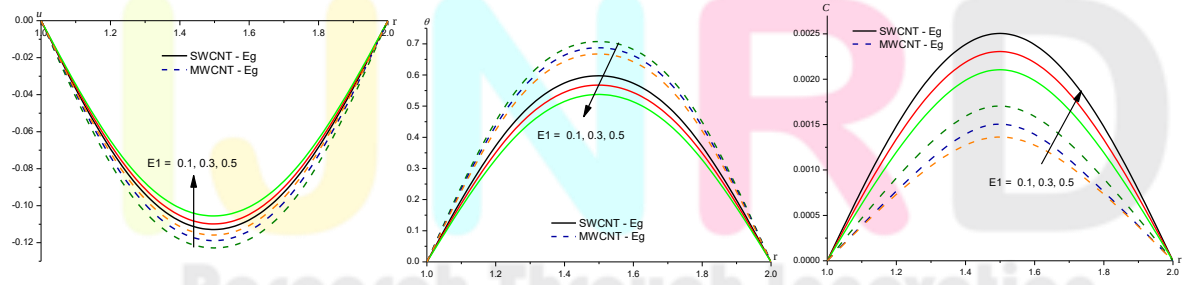

Fig.7 : Variation of [a] Velocity (u), [b] Temperature(θ), [c] Nanoconcentration(C) with E1
Rd=0.5, Ec=0.1, A11=0.1, B11=0.5, B=0.2, δ=0.1

Figs. 7(a)-7(c) exhibited the influence of activation energy parameter (E1). From the profiles we find that the velocity and temperature reduces and concentration enhances with higher values of 'E1'. This maybe due to the fact that the momentum and thermal boundary layer becomes thinner while solutal boundary layer becomes thicker with the increased in values of E1. The values of u and θ in Swcnt case are relatively smaller than those in Mwcnt case, while an opposite effect is observed in the behaviour of nanoconcentration.

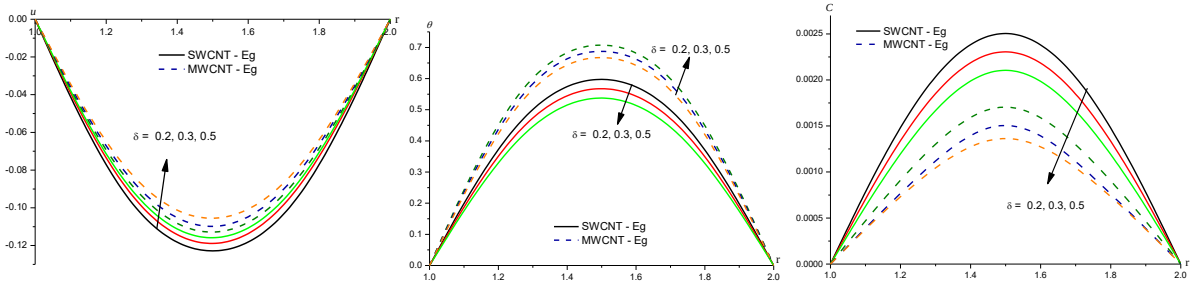

Fig.8 : Variation of [a] Velocity (u), [b] Temperature(θ), [c] Nanoconcentration(C) with δ
Rd=0.5, Ec=0.1, A11=0.1, B11=0.5, B=0.2, E1=0.1

Figs. 8(a)-8(c) represent (u,θ,C) with temperature difference ratio (δ) . The velocity and concentration depreciates with 'δ' in both types of nanofluids while the temperature reduces in Swcnt case and enhances in Mwcnt case. The values of u & C in Swcnt nanofluid are relatively greater than those in Eg-Swcnt nanofluid.

The sheer stress (τ) at the inner and outer cylinder (r = 1,2) have been shown in table 2 of different variations of Rd, Ec, A11, B11,E1, δ. From the tabular values we find that the stress decays at both the cylinder with increased in Radiation parameter (Rd)/ Eckert number (Ec) / space and temperature dependent heat source (A11,B11), Variable viscosity(B/ activation energy parameter (E1)/ temperature difference ratio (δ). From the above analysis, we find that the sheer stress at inner cylinder (r = 1) in Eg-SWCNT nanofluid are relatively lesser than those in Eg-MWCNT case. While an opposite effect is observed in the behaviour of (τ) at the outer cylinder (r = 2).

The local rate of heat transfer (Nusselt number) at the inner and outer cylinder (r = 1,2) have been shown in table 3 for a parametric variation. From the tabular values, we find that the Nusselt number reduces on inner cylinder (r = 1) and enhances outer cylinder (r = 2) with increase in radiation parameter (Rd)/ Eckert number (Ec)/ results in a depreciation in the Nusselt number at both the cylinders. The rate of heat transfer at both the cylinder experience enhancement with rising values of space and temperature dependent heat sources (A11,B11), activation energy parameter (E1)/ temperature difference ratio (δ). From the above analysis we find that the values of Nusselt number at both the cylinders in Eg-Swcnt nanofluid are relatively lesser than those in Eg-Mwcnt nanofluid.

The local rate of mass transfer (Sherwood number) is presented in table 4 for different values of E1. From the tabular values we find that lesser the molecular diffusivity (Ec)/ higher the activation energy (E1) larger the Sharwood number (Sh) at both the cylinder. Higher thermos-diffusion effects/ temperature difference ratio (δ) smaller the rate of mass transfer at both the cylinders. The rate of mass transfer decays at the inner cylinder (r = 1). From the above analysis we find that the values of rate of mass transfer at both cylinder (r = 1,2) in Eg-Swcnt nanofluid are relatively higher than those in Eg-Mwcnt case.

Table 2 : Skin friction(τ) & Nusselt number(Nu) with Swcnt-Eg and Mwcnt-Eg at r=1

Paramater		Eg-Swcnt		Eg-Mwcnt	
		τ(1)	**Nu(1)**	**τ(1)**	**Nu(1)**
B	0.25	-0.502712	-0.184469	-0.502928	-0.405918
	0.5	-0.502709	-0.184467	-0.502921	-0.405907
	1	-0.502706	-0.184465	-0.502914	-0.404602
A11	0.1	-0.502712	-0.184469	-0.502928	-0.405918
	0.3	-0.502709	-0.182568	-0.502921	-0.401729
	0.5	-0.502706	-0.180666	-0.502914	-0.400246
B11	0.3	-0.502712	-0.184469	-0.502928	-0.405918
	0.5	-0.502709	-0.184467	-0.502921	-0.405907
	1	-0.502706	-0.184465	-0.502914	-0.408602
Rd	0.5	-0.502712	-0.184469	-0.502928	-0.405918
	1.5	-0.502714	-0.102477	-0.502927	-0.225483
	5	-0.502716	-0.040093	-0.502930	-0.088787
Ec	0.05	-0.502712	-0.184469	-0.502928	-0.405918
	0.1	-0.502706	-0.304786	-0.502914	-0.670669
	0.2	-0.502697	-0.425090	-0.502892	-0.943638
E1	0.3	-0.502712	-0.184468	-0.502928	-0.405917
	0.5	-0.502709	-0.184467	-0.502921	-0.405907
	0.7	-0.502706	-0.184465	-0.502914	-0.405615
δ	0.1	-0.502712	-0.184469	-0.502928	-0.405918
	0.2	-0.502709	-0.184467	-0.502921	-0.405907
	0.3	-0.502706	-0.184464	-0.502914	-0.405601

Table 3 : Skin friction(τ) & Nusselt number(Nu) with Swcnt-Eg and Mwcnt-Eg at r= 2

Paramater		Eg-Swcnt		Eg-Mwcnt	
		τ(2)	Nu(2)	τ(2)	Nu(2)
B	0.25	0.487243	0.181037	0.487019	0.398150
	0.5	0.487240	0.181034	0.487012	0.398139
	1.0	0.487237	0.181032	0.487005	0.317827
A11	0.1	0.487243	0.181037	0.487019	0.398150
	0.3	0.487240	0.179147	0.487012	0.393988
	0.5	0.487238	0.177258	0.487006	0.392526
B11	0.3	0.487243	0.181037	0.487019	0.398150
	0.5	0.487240	0.181034	0.487012	0.398139
	1.0	0.487237	0.181032	0.487005	0.397629
Rd	0.5	0.487243	0.181037	0.487019	0.398150
	1.5	0.487245	0.100571	0.487018	0.221169
	5.0	0.487254	0.094561	0.487011	0.112569
Ec	0.05	0.487243	0.181037	0.487019	0.398150
	0.1	0.487237	0.298431	0.487005	0.656288
	0.2	0.487229	0.415812	0.486984	0.922621
E1	0.3	0.487243	0.181036	0.487019	0.398149
	0.5	0.487240	0.181034	0.487012	0.398042
	0.7	0.487237	0.181031	0.487005	0.400843
δ	0.1	0.487243	0.181037	0.487019	0.398150
	0.2	0.487240	0.181034	0.487012	0.398739
	0.3	0.487237	0.181032	0.487005	0.400828

Table 4 : Sherwood number with Swcnt-Eg and Mwcnt-Eg at r=1 & 2

Parameter		Eg-Swcnt		Eg-Mwcnt	
		Sh(1)	Sh(2)	Sh(1)	Sh(2)
B	0.25	-0.895775	0.882346	-0.895351	0.881779
	0.5	-0.895763	0.882345	-0.895337	0.881766
	3	-0.895757	0.882334	-0.895314	0.881743
A11	0.1	-0.895775	0.882346	-0.895351	0.881779
	0.3	-0.895767	0.882344	-0.895346	0.881774
	0.5	-0.895766	0.882342	-0.895332	0.881766
B11	0.3	-0.895775	0.882346	-0.895351	0.881779
	0.5	-0.895763	0.882345	-0.895336	0.881765
	1	-0.895757	0.882333	-0.895312	0.881745
Rd	0.5	-0.895775	0.882346	-0.895351	0.881779
	1.5	-0.895947	0.882519	-0.895742	0.882161
	5	-0.896086	0.882655	-0.896047	0.882457
Ec	0.05	-0.895775	0.882346	-0.895351	0.881779
	0.1	-0.895494	0.882078	-0.894743	0.881189
	0.2	-0.895213	0.881804	-0.894097	0.880566
E1	0.2	-0.894109	0.880705	-0.893691	0.880139
	0.4	-0.897271	0.883829	-0.896843	0.883254
	0.6	-0.899875	0.886403	-0.899429	0.885808
δ	0.1	-0.895778	0.882346	-0.895351	0.881779
	0.3	-0.895763	0.882348	-0.895336	0.881765
	0.5	-0.895757	0.882333	-0.895315	0.881743

7. CONCLUSIONS

The non-linear, coupled equations governing the flow have been solved by numerical methods. From the variations of velocity, temperature and nanoconcentration with different parameters, we conclude that

- Increase in space and temperature dependent heat source parameters (A11,B11)/viscosity parameter (B) decays the velocity, temperature and nanoconcentration in the flow field in both types of nanofluid.
- Increase in Ec upsurges the temperature depreciates the velocity, nanoconcentration.
- Higher thermal radiation (Rd) larger velocity, nanoconcentration,depreaciates the temperature in the flow.
- Increase in Activation energy (E1) reduces velocity, temperature and enhances the nanoconcentration.
- Increase in temperature difference ratio (δ) smaller the velocity, nanoconcentration while the temperature reduces in SWCNT case and enhances in MWCNT case.

8. REFERENCES

[1]. Abu-Nada Eiyad , Masoud Ziyad N., Hijazi Ala L. Natural Convection Heat Transfer Enhancement in Horizontal Concentric Annuli Using Nanofluids, May 2008, International Communications in Heat and Mass Transfer 35(5):657-665, DOI:10.1016/j.icheatmasstransfer.2007.11.004

[2]. Abu-Nada Eiyad: Effects of Variable Viscosity and Thermal Conductivity of CuO-Water Nanofluid on Heat Transfer Enhancement in Natural Convection: Mathematical Model and Simulation, May 2010, Journal of Heat Transfer 132(5):052401, DOI:10.1115/1.4000440

[3]. Al-Marri J., Ismail W. Almanassra , Ahmed Abdala , Muataz A. Atieh , Heat transfer enhancement of nanofluids using iron nanoparticles decorated carbon nanotubes, Appl. Thermal Eng. 107 (25) (2016) 1008–1018.

[4]. Amotosh Tiwari : : activation energy impacts on hydromagnetic convective heat transfer flow of nanofluid past a surface of vertical wavy with variable properties, *International Journal of Computer Applications (0975 – 8887)* (2023)*Volume 184 – No. 50*, www.ijcaonline.org

[5]. Arash Karimipour , Abdolmajid Taghipour , Amir Malvandi , Developing the laminar MHD forced convection flow of water/FMWNT carbon nanotubes in a microchannel imposed the uniform heat flux, J. Magn. Magn. Mater. 419 (2016) 420–428 .

[6]. Berrehal H. and Maougal A., "Entropy generation analysis for multi-walled carbon nanotube (MWCNT) suspended nanofluid flow over wedge with thermal radiation and convective boundary condition," *Journal of Mechanical Science and Technology*, vol. 33, no. 1, pp. 459–464, (2019).

[7]. Buongiorne,J:Convective transport in Nanofluids,Journal Heat transfer 128,pp.250-250(2006)

[8]. Choi S.U.S and Eastman,A:Enhancinh thermal conductivity of fluids with Nanoparticles,ASME publications-Fed231,pp.99-106(1995)

[9]. Devasena Y: effect of non-linear thermal radiation, activation energy on hydromagnetic convective heat and mass transfer flow of nanofluid in vertical channel with Brownian motion and thermophoresis in the presence of irregular heat sources, *World Journal of Engineering Research and Technology* (JERT) *wjert,* (2023), *Vol. 9, Issue 2, XX-XX,* ISSN 2454-695X, SJIF Impact Factor: 5.924, www.wjert.org

[10]. Kamali R, Binesh A : Numerical investigation of heat transfer enhancement using carbon nanotube-based non-Newtonian nanofluids, Int. Commun. Heat Mass Transf. Vol.37(8), pp.1153–1157, (2010)

[11]. Kathyani,G and Venkata Subrahmanyam,P:Effect of dissipation on HD convective heat and mass transfer flow of thermally radiating nanofluid in vertical channel with activation energy and irregular heat sources.,MukthShabd Journal,ISSN No.2347 -3150,Scientific Journal;ISSN No:2347-3150, Vol.XII,Issue.III, March (2023) pp.433-441

[12]. Kiran Kumar T,Srinivasa Rao P, and MD. Shamshuddin, "Effect of thermal radiation on nonDarcy hydromagnetic convective heat and mass transfer flow of a water -SWCNT's and MWCNT's nanofluids in a cylindrical annulus with thermo-diffusion and chemical n reaction. International Journal of Modern Physics B, Vol. 38, No. 01, 2450011 (2024), https://doi.org/10.1142/S0217979224500115.

[13]. Kumaresan V, Khader SMA, Karthikeyan S, Velraj R. Convective heat transfer characteristics of CNT nanofluids in a tubular heat exchanger of various lengths for energy efficient cooling/heating system. International Journal of Heat and Mass Transfer. 2013;60:413-421

[14]. Maria Imtiaz , Tasawar Hayat , Ahmed Alsaedi , Bashir Ahmad , Convective flow of carbon nanotubes between rotating stretchable disks with thermal radiation effects, Int. J. Heat Mass Transf. 101 (2016) 948–957.

[15]. Mehdi Nojoomizadeh , Arash Karimipour , The effects of poros- ity and permeability on fluid flow and heat transfer of multi walled carbon nano-tubes suspended in oil (MWCNT/oil nano-fluid) in a microchannel filled with a porous medium, Phys. E: Low-dimensional Syst. Nanostrut. 84 (2016) 423–433.

[16]. Nagasasikala M : Effect of activation energy on convective heat and mass transfer flow of dissipative nanofluid in vertical channel with Brownian motion and thermophoresis in the presence of irregular heat sources, *World Journal of Engineering Research and Technology* (JERT) *wjert, , Vol. 9, Issue 2,* (2023) *XX-XX,* ISSN 2454-695X, SJIF Impact Factor: 5.924, www.wjert.org

[17]. Oztop H. F. and Abu-Nada E., "Numerical study of natural convection in partially heated rectangular enclosures filled with nanofluids," *International Journal of Heat and Fluid Flow*, vol. 29, no. 5, pp. 1326–1336, (2008).

[18]. Satya Narayana K and Ramakrishna G N : Effect of variable viscosity, activation energy and irregular heat sources on convective heat and mass transfer flow of nanofluid in a channel with brownian motion and thermophoresis, *World Journal of Engineering Research and Technology* (WJERT), (2023), *Vol. 9, Issue 2, XX-XX,* ISSN 2454-695X, SJIF Impact Factor: 5.924, www.wjert.org

[19]. Shafiq A., Khan I., Rasool G., Sherif E. M., and Sheikh A. H., "Influence of single- and multi-wall carbon nanotubes on magnetohydrodynamic stagnation point nanofluid flow over variable thicker surface with concave and convex effects," *Mathematics*, vol. 8, no. 104, (2020).

[20]. Shahsavar A., Saghafian M., Salimpour M.R., Shafii M.B., Experimental investigation on laminar forced convective heat transfe r of ferrofluid loaded ith carbon nanotubes under con- stant and alternating magnetic fields, Exp. Thermal Fluid Sci 76 (2016) 1–11.

[21]. Svante Arrhenius "Activation Energy and the Arrhenius Equation – Introductory Chemistry- 1st Canadian Edition". opentextbc.ca. Archived from the original on 2017-07-08. Retrieved 2018-04-05.

[22]. Tao, L.N: On combined and forced convection in channels, ASME J. Heat Transfer, V.82, 233-238(1960).

[23]. Tiwari R. K. and Das M. K.: "Heat transfer augmentation in a two-sided lid-driven differentially heated square cavity utilizing nanofluids," *International Journal of Heat and Mass Transfer*, vol. 50, no. 9-10, pp. 2002–2018, (2007).

[24]. Vijayalakshmi,P:Effect of thermal radiation on non-darcy hydromagnetic convective heat and mass transfer flow of water-swcnt's nanofluid in a cylindrical annulus with thermo-diffusion and chemical reaction ,Journal of Xi's University of Archetecture and Technology,Issn No.1006-7930,V.Xiii,Issue.3,pp.16-29(2021)